Inverse Problems in Engineering: Theory and Practice:
3rd Int. Conference on Inverse Problems in Engineering
June 13-18, 1999, Port Ludlow, WA

HT20

A BOUNDARY INVERSE HEAT CONDUCTION PROBLEM WITH PHASE CHANGE FOR MOISTURE-BEARING POROUS MEDIUM

Keith A. Woodbury
Mechanical Engineering Department
University of Alabama
Tuscaloosa, AL 35487

Quanpeng Ke
Mechanical Engineering Department
University of Alabama
Tuscaloosa, AL 35487

ABSTRACT

Heat flux at the mold/metal interface is an important parameter in the casting process. Measurement of this heat flux during casting with green sand molds is complicated by the presence of moisture in the sand. It is desired to accurately estimate the heat flux during green sand casting in order to improve numerical simulations and, ultimately, casting quality.

In this paper, a zonal model of the moisture movement in moisture-bearing sand (Tsai, et al., 1986) is incorporated into an inverse solution procedure to determine the mold/metal interface heat flux. The inverse method uses an iterative Gaussian update algorithm (Beck and Arnold, 1977, pg. 341) (Junkins, 1978, pg. 33) to estimate the heat flux.

A sensitivity analysis shows that the sensors must be located near the surface. A numerical experiment confirms the utility of this algorithm as the result is in good agreement with the exact data.

NOMENCLATURE

ENGLISH

C_d	specific heat of dry sand
C_w	specific heat of water
K_2	thermal conductivity of dry sand
L	latent heat of water vaporization
P	matrix defined by Eq.(6-b)
q	unknown heat flux
s	sum of weighted square error
t	time
T_1	temperature of castings
T_2	temperature of dry sand zone
T_{2i}	initial temperature of dry sand
T_c	vaporization temperature of water
U	weighting matrix
W	moisture content in vapor transportation zone
W_0	initial sand moisture content
W	weighting matrix
X	sensitivity coefficient matrix
Y	measured system response vector

GREEK

ζ_1	position of vaporization interface
ζ_3	position of condensation interface
α_2	thermal diffusivity of dry sand
ρ_2	density of dry sand
$\boldsymbol{\beta}$	unknown parameter vector
$\boldsymbol{\eta}$	calculated system response vector
$\boldsymbol{\mu}$	parameter vector known from prior information

SUBSCRIPTS / SUPERSCRIPTS

1	parameters of castings
2	parameters of dry sand zone
3	parameters of vapor transportation zone
4	parameters of external zone
e	element
k	iteration index

INTRODUCTION

Heat flux is one of the most important parameters influencing the process of solidification of metal in a green sand mold. Many casting defects, such as scab, vein, buckle, rat tail, spalling etc, are caused by excessive heat flux. Precise determination of the heat flux is a key factor in realizing precision casting.

The problem of heat flux determination in green sand is complicated by the presence of three zones formed when molten

Copyright © 1999 by ASME

metal is poured into the mold. Moisture in the sand mold near the metal-sand interface flashes into vapor and the vapor moves away from the metal and penetrates further into the sand mold. If the sand mold is thick enough, the vapor will condense where the temperature is low. Thus the entire sand mold has three distinct regions: the dry sand zone, the vapor transportation zone, and the external zone. In each zone, the temperature distribution is quite different.

Many authors (Tsai, et al. (1986), Marek (1963), Marek (1965), Chowdialh (1973), Draper (1969)) have investigated the zonal models in sand to predict the transient temperature distribution and the movement of vapor. However, as far as the authors can determine, there are no papers solving the Inverse Heat Conduction Problem to find the heat flux using a zonal model.

In this paper, the authors develop an inverse heat conduction problem algorithm to find the surface heat flux in green sand molds. In the following sections, the forward solver is reviewed. Next, this forward solver is incorporated into the inverse algorithm which uses Gauss's iterative minimization scheme. The sensitivity coefficients are directly calculated from a sensitivity model developed by the authors using the finite element method. A numerical experiment is conducted and it is shown that when the sensor is located at the surface, this method gives an excellent result. If the sensor is located close to the surface, this algorithm can give reasonable results.

THE FORWARD MODEL

As the first step to construct the inverse problem algorithm, let us consider the mathematical description of the forward problem.

The zonal model is stated in detail by Tsai, et al. (1986). Figure 1 shows the different regions in green sand. The analysis for each of these zones is described below.

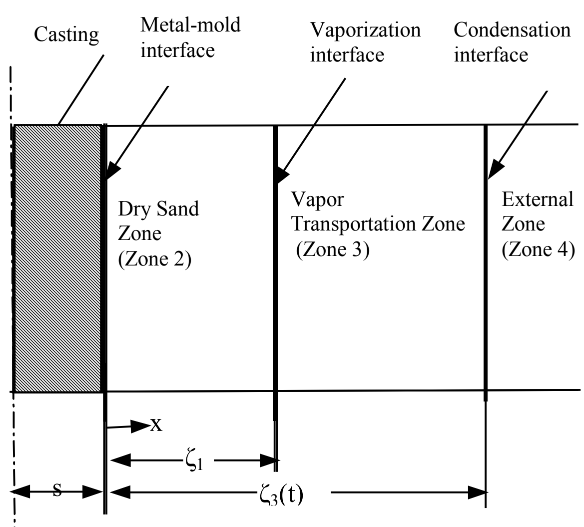

Fig 1 Schematic representation of different zones in green sand

In zone 1, the molten metal will solidify and release heat. This heat release is not important in the inverse algorithm, so its description is omitted here. Details are available in Tsai, et al. (1986).

In zone 2, the dry sand zone, simple one dimensional transient heat conduction problem must be solved, but the location of the right boundary location will change with time. The mathematical description for this zone is:

$$C_2(T)\frac{\partial T_2}{\partial t} = k_2(T)\frac{\partial^2 T_2}{\partial x^2} \qquad \text{in } 0 \le x \le \zeta_1(t) \tag{1-a}$$

$$-k_2\frac{\partial T_2}{\partial x} = q(t) \qquad \text{on } x=0 \tag{1-b}$$

$$T_2 = T_c \qquad \text{on } x=\zeta_1(t) \tag{1-c}$$

$$-k_2\frac{\partial T_2}{\partial x} = L\rho_2 W\frac{\partial \zeta_1}{\partial t} \qquad \text{on } x=\zeta_1(t) \tag{1-d}$$

In zone 3, the vapor transportation zone, the temperature remains constant and the governing equation in this zone is simple,

$$T_3 = T_c\,, \tag{2}$$

where T_c is vaporization temperature of water.

The water content in the vapor transportation zone is assumed to be:

$$W = W_0 + \{W_0 C_W + (100 - W_0)C_d\}(T_c - T_{2i})/L\,. \tag{3}$$

Using an energy balance equation, the vapor transportation interface can be calculated from

$$\zeta_3(t) = \frac{W}{W - W_0}\zeta_1(t)\,. \tag{4}$$

The external zone can be treated as a semi-infinite region. However, it is not important in the inverse algorithm as the sensor can not be located in this zone. The reason for this will be given later in this paper.

THE INVERSE METHOD

The inverse problem scheme is presented in the Fig 2, where transient heat conduction in the dry sand zone is considered. It is assumed that all the boundary conditions are known except the mold/cast interface heat flux, which is a function of time and which should be identified. It is also assumed that the thermophysical properties, which may be temperature dependent, are exactly known. Several thermocouples may be located in the mold to measure the transient temperature at those points. The results of these measurements are used to solve the inverse problem to find the heat flux between castings and the dry sand mold.

The objective function used in Gaussian iterative updating method (Beck and Arnold, 1977) is

$$S = [\mathbf{Y} - \boldsymbol{\eta}(\boldsymbol{\beta})]^T \mathbf{W}[\mathbf{Y} - \boldsymbol{\eta}(\boldsymbol{\beta})] + (\boldsymbol{\mu} - \boldsymbol{\beta})^T \mathbf{U}(\boldsymbol{\mu} - \boldsymbol{\beta}) \tag{5}$$

Where S is the weighted sum of square errors, **W** and **U** are weighting matrix, **Y** is the measurement temperature and $\boldsymbol{\eta}(\boldsymbol{\beta})$ is the calculated response (temperature) using the estimated

Copyright © 1999 by ASME

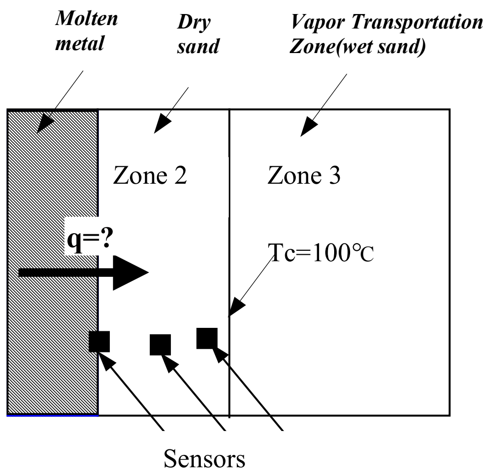

Fig 2 Graphic representation of the inverse problem

parameters (heat flux). Taking the derivative of Eq.(5) with respect to the unknown parameters and expanding the response with a Taylor's series and introducing the sensitivity coefficient results the following iterative formula to correct the initial guess,

$$\mathbf{b}^{(k+1)} = \mathbf{b}^{(k)} + \mathbf{P}^{(k)}[\mathbf{X}^{(k)T}\mathbf{W}(\mathbf{Y}-\boldsymbol{\eta}^{(k)}) + \mathbf{U}(\boldsymbol{\mu}-\mathbf{b}^{(k)})] \quad (6\text{-a})$$

$$\left[\mathbf{P}^{(k)}\right]^{-1} = \mathbf{X}^{T(k)}\mathbf{W}\mathbf{X}^{(k)} + \mathbf{U} \quad (6\text{-b})$$

The sensitivity coefficient takes the following form:

$$\mathbf{X} = \begin{bmatrix} X_{11} & \cdots & X_{1p} \\ \vdots & \ddots & \vdots \\ X_{n1} & \cdots & X_{np} \end{bmatrix} = \begin{bmatrix} \frac{\partial\eta_1}{\partial\beta_1} & \cdots & \frac{\partial\eta_1}{\partial\beta_p} \\ \vdots & \ddots & \vdots \\ \frac{\partial\eta_n}{\partial\beta_1} & \cdots & \frac{\partial\eta_n}{\partial\beta_p} \end{bmatrix} \quad (7)$$

In this specific case, $\boldsymbol{\eta}$ is replaced by $\mathbf{T}$, the computed temperatures from Eq.(1) and $\boldsymbol{\beta}$ is replaced by $\mathbf{q}$, a vector of $\{q_1, q_2, \cdots, q_r\}$ components over "*r*" time steps. The result is:

$$\mathbf{X} = \begin{bmatrix} \frac{\partial T_1}{\partial q_1} & \cdots & \frac{\partial T_1}{\partial q_r} \\ \vdots & \ddots & \vdots \\ \frac{\partial T_n}{\partial q_1} & \cdots & \frac{\partial T_n}{\partial q_r} \end{bmatrix}. \quad (8)$$

Assuming $q_1 = q_2 = \cdots = q_r = q_0$ over the "*r*" future time steps (Beck et al,1985). In each time step, only one unknown heat flux is estimated and all the heat fluxes are estimated sequentially. By doing this, Eq(8) can be written as

$$\mathbf{X} = \begin{bmatrix} \frac{\partial T_1}{\partial q_0} & \cdots & \frac{\partial T_1}{\partial q_0} \\ \vdots & \ddots & \vdots \\ \frac{\partial T_n}{\partial q_0} & \cdots & \frac{\partial T_n}{\partial q_0} \end{bmatrix} \quad (8')$$

SENSITIVITY COEFFICIENTS ANALYSIS

Sensitivity coefficients are obviously important parameters in the IHCP. In this section, the finite element method to find the sensitivity coefficients is derived directly from the mathematical description of the governing equation in the dry sand zone. The governing equations for heat transfer in the dry sand zone are given in Eq (1).

Taking the derivative of equation (1-a) through (1-c) with respect to q_0, and assuming the constant thermal physical properties in each element, but they will change from element to element (Chen, 1997), we have

$$C_2 \frac{\partial X}{\partial t} = \frac{\partial}{\partial x}\left(k_2 \frac{\partial X}{\partial x}\right) \qquad \text{in } 0 \le x \le \zeta_1(t) \quad (9\text{-a})$$

$$-k_2 \frac{\partial X}{\partial x} = 1 \qquad \text{on } x = 0 \quad (9\text{-b})$$

$$X = 0 \qquad \text{on } x = \zeta_1(t) \quad (9\text{-c})$$

The Galerkin method of weighted residuals expression for the sensitivity coefficient is

$$\int_{x_1}^{x_2} N_i \left[\frac{\partial}{\partial x}\left(k_x^{(e)}(T) \frac{\partial X_{q_0}}{\partial x}\right) - C_x^{(e)}(T) \frac{\partial X_{q_0}}{\partial t}\right] dx = 0 \quad (10\text{-a})$$

$$-k_x^{(e)}(T) \frac{\partial X_{q_0}(0,t)}{\partial x} = 1 \quad (10\text{-b})$$

$$-k_x^{(e)}(T) \frac{\partial X_{q_0}(L,t)}{\partial x} = 0 \quad (10\text{-c})$$

By assuming $k_x^{(e)}$ and $C_x^{(e)}$ constant in each element and integrating by parts, the following finite element equations result

$$[C]\{\dot{X}\} + [K]\{X\} = \{R_q\} \quad (11\text{-a})$$

$$[C] = \frac{C_x^{(e)} l_e}{6} \begin{bmatrix} 2 & 1 \\ 1 & 2 \end{bmatrix} \quad (11\text{-b})$$

$$[K] = \frac{k_x^{(e)}}{l_e} \begin{bmatrix} 1 & -1 \\ -1 & 1 \end{bmatrix} \quad (11\text{-c})$$

$$\{R_q\} = \begin{cases} \begin{Bmatrix} 1 \\ 0 \end{Bmatrix} & \text{for element 1} \\ \begin{Bmatrix} 0 \\ 0 \end{Bmatrix} & \text{for all other elements} \end{cases} \quad (11\text{-d})$$

The sensitivity coefficient is solved directly and the results are shown in Fig 3 and Fig 4. Fig 3 shows sensitivity coefficients for sensors at 0 mm, 1 mm, 3 mm, 5 mm and 10 mm below the surface and a heat flux of 20,000 W/m^2. Fig 4 shows sensitivity coefficients for sensors at 0 mm, 1 mm, 3 mm, 5 mm and 10 mm and a heat flux of 200,000 W/m^2. At a specific time, the sensitivity coefficient at the left surface where heat is added is larger than anywhere else. For sensor locations farther away from that surface, the sensitivity coefficient will decrease.

Copyright © 1999 by ASME

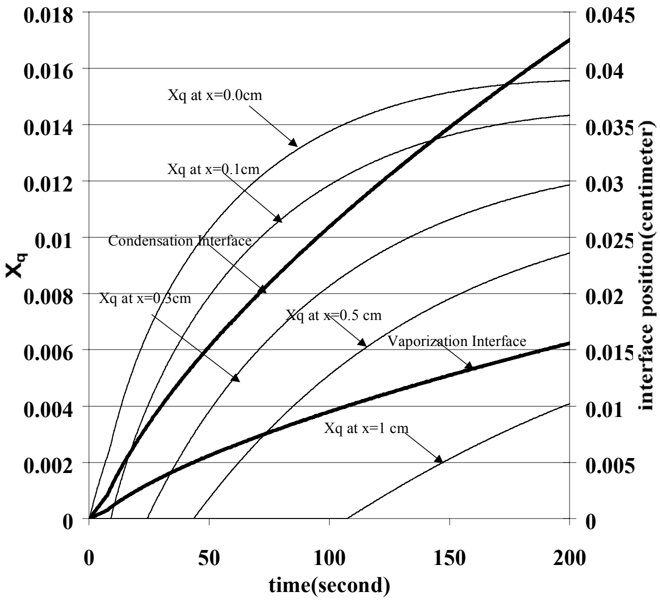

Figure 3 sensitivity coefficient at different sensor locations when q=20,000W/m^2

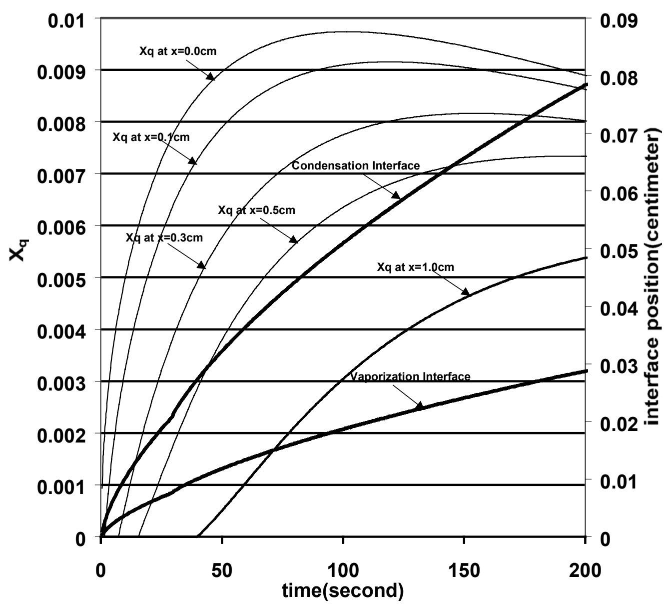

Figure 4. sensitivity coefficient at different sensor locations when q=200,000W/m^2

A very important phenomena inherent to moisture-bearing porous media is that the sensitivity coefficient will be zero for some time for sensor locations away from the heated surface. This is seen in Fig 3 and 4 for the subsurface sensors. It makes the inverse algorithm very challenging. The reason for this phenomenon is the presence of the vaporization region that masks the effect of surface heat flux. As heat is added continuously to green sand, the vaporization interface and the condensation interface will move with time. The locations of these fronts at each time are also shown in Fig 3 and 4.

The reason for the initial zero value of **X** for subsurface sensors can be shown as follows.

At first, the sensor will be in the external zone. In this zone, the mathematical descriptions are :

$$\frac{\partial T_4}{\partial t} = \alpha_4 \frac{\partial^2 T_4}{\partial x^2} \qquad \text{in } \zeta_2(t) \le x \le \infty \qquad (12\text{-a})$$

$$T_4 = T_c \qquad \text{on } x = \zeta_2(t) \qquad (12\text{-b})$$

$$T_4 = T_i \qquad \text{on } x = \infty \qquad (12\text{-c})$$

It contains no information about the left boundary heat flux. The derivative of the above equations with respect to q_0 is zero, this means the temperature is independent of the heat flux, so X_{q_0} is zero.

As the condensation interface moves and reaches the sensor location, the sensor will fall into the vapor transport zone. In this zone, no matter how large the heat flux is, the temperature still remains constant. Its value is equal to the vaporization temperature of water, so that the temperature is also independent of the heat flux added at the left boundary and the sensitivity remains zero. Only after the vaporization interface passes over the sensor will the sensor be located in the dry sand zone and from then on, the sensitivity will be non-zero and it will increase with time. Fig 3 and 4 clearly show this. If there is no sensitivity, then there is no information about the heat flux.

In summary, the best place for the sensor to be located is on the active surface. If the sensor is located below the surface, there will be a period of time (proportional to the depth of the sensor) when no information about heat flux is available. There will be loss of information of the heat flux until the sensor falls into the dry sand zone.

ESTIMATION PROCEDURES

The heat flux components are estimated sequentially according to the following algorithm.

1. assume an initial guess for q_0.
2. use equation (1-d) to find the domain length.
3. use the calculated first domain length and the assumed heat flux to solve the governing equations (1-a) to (1-c) to find temperature at the left surface.
4. solve the sensitivity coefficient equations (9-a) to (9-c) to get the sensitivity coefficients
5. using Gaussian iterative method—equations (6-a) and (6-b) to solve new heat flux
6. repeat process 2 to 5 until Δq is “very small”.
7. increase time by one time step, repeat process 1 to 6 sequentially to estimate all the heat flux components each time.

Copyright © 1999 by ASME

TEST CASES AND RESULT

To illustrate the validity of the present inverse algorithm with phase change for moisture-bearing porous medium in identifying the heat input at the surface from the knowledge of the temporal temperature recordings, we consider a specific example where the heat flux at the boundary is given as:

$$q_0 = \begin{cases} 500 + 1950\,t & 0 \le t \le 10 \\ 20000 - 500(t-10) & 10 \le t \le 50 \\ 0 & t > 50 \end{cases} \qquad (13)$$

where the unit for time is second and the unit for heat flux is W/m^2. This heat flux is used with the forward model of Tsai, et al (1986) to generate some "artificial data". This data is subsequently used in the inverse algorithm, and the results of the inverse solution can be compared back to the original heat flux (Eq. (13)).

The objective of this article is to show the validity and accuracy of the algorithm developed above to estimate the unknown heat flux with no prior information on the functional form of the unknown quantities. Five cases are presented here. The first two are for cases that the sensor is located at the left boundary, the last three are for the case that the sensor is located at the subsurface.

In order to compare the result for situations involving random measurement errors, we assume normally distributed uncorrelated errors with zero mean and constant standard deviation. Both the simulated exact and inexact measurement data can be expressed as

$$\mathbf{Y} = \mathbf{Y}_{exact} + \omega\sigma$$

where $\mathbf{Y}_{\mathrm{exact}}$ is the solution of the direct problem with an exact heat flux given by equation (13), σ is the standard deviation of the measurement, and ω is a random variable. The variable ω is from a normal distribution with zero mean and unity variance and is generated by a subroutine named RANDOM.C (Press et al., 1993).

In all these tests, the initial temperature is 25 ˚C and the initial water content is 5%.

For test case 1, there is no error added (σ=0). The sensor is located at the surface where the heat acts. Fig 5 shows the results from this test case. It can be seen from Fig 5 that the estimated data are in very good agreement with the exact heat flux except some loss of q near the peak.

In test case 2, 5% random error $\left(\sigma = \dfrac{0.05 \cdot T_{\max}}{1.96}\right)$ is added and the sensor is also located at the surface. The results are shown in Fig 6. The estimated data is also in good agreement with the exact heat flux although there is some obvious departure from exact data around the peak heat flux. This deviation is inherent to the sequential estimation and can be reduced to some extent by the used of smaller "r", provided that stable results can be achieved. From the results of these two test cases, one conclusion that can be made is that if the sensor is located at the surface, this algorithm can work well in identifying the unknown heat flux in green sand.

However, in practice, it is difficult to attach a thermal sensor integral to the surface of the green sand. The effect of subsurface sensors on the estimated heat flux is investigated next.

Fig 7 shows the results when the sensor is located at 0.5 mm below the active boundary and the initial guess for the unknown heat flux is 9000 W/m^2. Also shown for reference in Fig 7 is the temperature input for the inverse algorithm. From Fig 7 one can see a peculiar phenomena. During the first 7 seconds, the heat flux remains constant and is equal to the initial guess. As stated in the sensitivity analysis section, during this period, the sensor is located first in the external zone and then

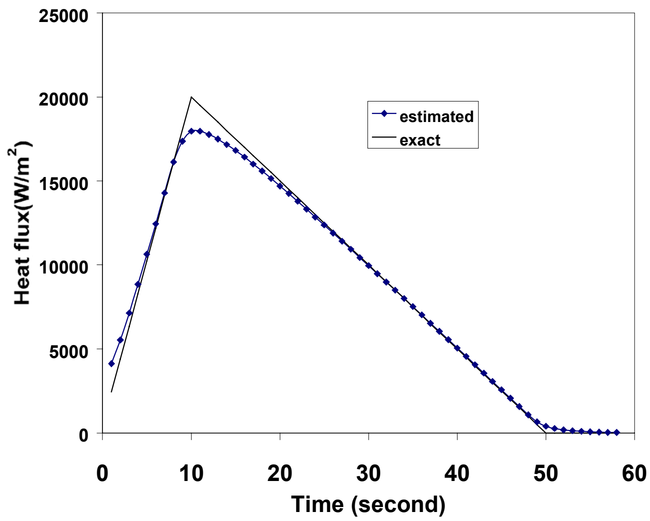

Fig 5. Test case 1, heat flux using exact data with r=3 and time step from data=1.0 s

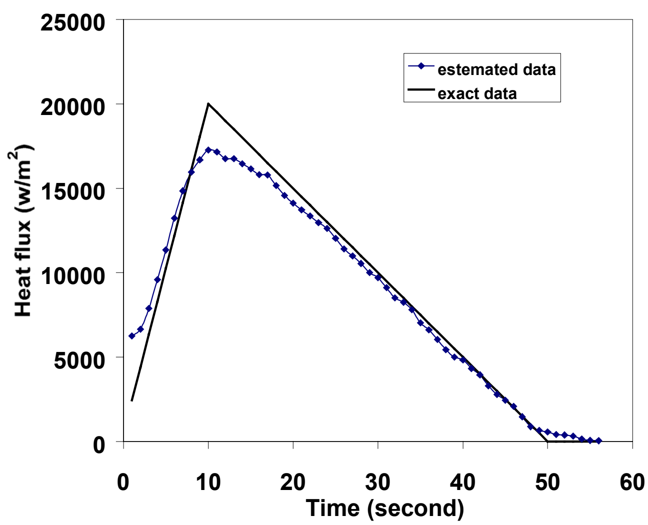

Figure 6. Test case 2, heat flux using data with simulated error (5%), r=5, time step in data = 1.0 s

Copyright © 1999 by ASME

in the vapor transportation zone. The sensitivity coefficients are zero in both of these two zones. Since the sensitivity coefficients are zero, we have no information about the heat flux, so we can not make adjustment to the initial guess until the sensitivity coefficients are nonzero.

The time requirement for the sensor to appear in the dry sand region can be observed from the temperature data in Fig 7. This time is about 7 seconds. Note that the time required for the "sensor" in the model to appear in the dry sand zone is also about 7 seconds, as evidenced by the heat flux in Fig 7. So one

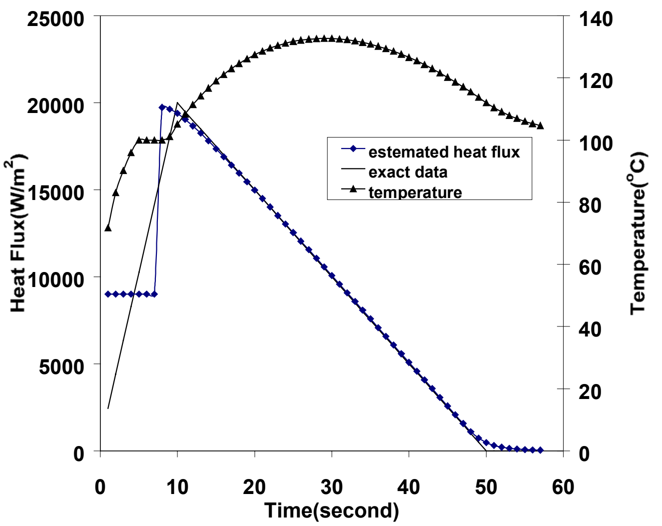

Fig 7 Test case 3. Heat flux using exact data with r=4 and time step from data =1.0 second, sensor located at 0.5 mm from the left surface, initial guess 9000 W/m^2

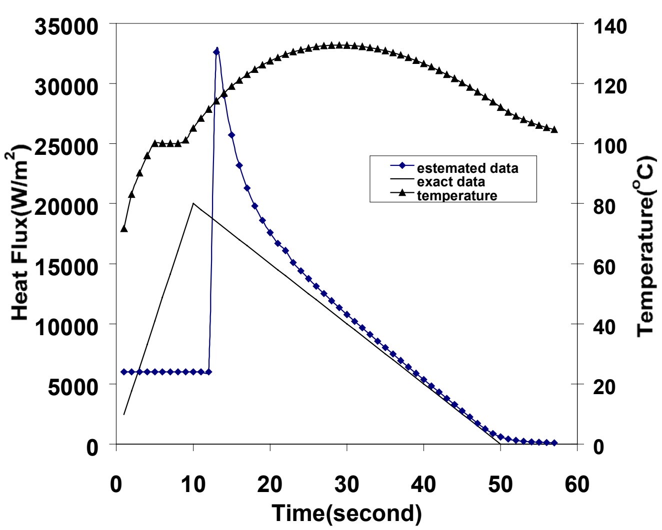

Fig 8 test case 4. Heat flux using exact data with r=4 and time step from data =1.0 second, sensor located at 0.5 mm from the left surface, initial guess 6000 W/m^2

can conclude that the initial guess for the heat flux ($q_0 = 9000$ W/m^2) is appropriate for this case. Fig 7 shows that the estimated data is in good agreement with the exact heat flux after the sensor is located at the dry sand (7 seconds later).

Fig 8 shows the results when the sensor is located at 0.5 mm below the active boundary and the initial guess is 6000 W/m^2. Using this guess, it takes too long for the sensor to appear in the dry sand zone. From the simulated temperature distribution in Fig 8, the sensor will be located at the dry sand zone after 7 seconds, but from the calculated heat flux history, the sensor will be not appear in the dry sand zone until time equals 13 seconds. This suggests that the initial guess of 6000 W/m^2 is too low for this case.

Fig 9 shows the result of the case when the initial guess (12000 W/m^2) is high. It is clear that the initial guess is too large because the calculated time for sensor to be located at the dry sand zone is 4 seconds, but the time for sensor to be located at the dry sand zone from the temperature data is 7 seconds. Also shown in Fig 9 is the existence of a second flat region for the estimated heat flux. The existence of this flat region is because of the difficulty of convergence after the initial guess is too high. For these overly high (case 5) or overly low (case 4) initial guesses, there exists large difference between the estimated result and the exact heat flux. These initial guesses can not be used to identify the surface heat flux in green sand.

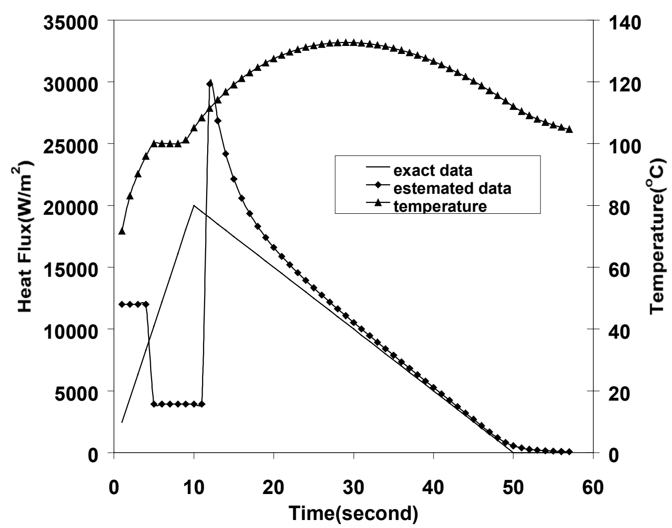

Fig 9 Test case 5. Heat flux using exact data with r=4 and time step from data =1.0 second, sensor located at 0.5 mm from the left surface, initial guess 10000 W/m^2

From the results of the 5 test cases, we can certify the accuracy of the sensitivity analysis and the validity of the inverse algorithm developed in this paper. When the sensor is located at the surface, it is not difficult to estimate the boundary heat flux and we lose no information about the heat flux history.

Copyright © 1999 by ASME

But when the sensor is located at the subsurface, there exists a “blind time” when there is no information about the heat flux. The length of this “blind time” is proportional to the depth of the sensor. This makes the inverse algorithm complicated and the result depends heavily on the initial guess. A too high or too low initial guess can not be used to track the right heat flux history, but good results still can be achieved if the initial guess is chosen carefully according to the criteria given in this paper.

CONCLUSION

A zonal model of the moisture movement in moisture-bearing sand is incorporated into an inverse solution procedure to determine the mold/metal interface heat flux. The inverse method uses an iterative Gaussian update algorithm to estimate the heat flux.

A sensitivity analysis shows that the sensors must be located near the surface. A numerical experiment confirms the utility of this algorithm as the result is in good agreement with the exact data. The choice of initial guess for the algorithm is important and the magnitude of the initial guess should be chosen by considering the temperature data.

ACKNOWLEDGMENTS

Work supported by the U.S. Department of Energy, Assistant Secretary for Conservation and Renewable Energy, Office of Industrial Technologies, under Cooperative Agreement DE-FC07-95ID13363, the American Foundrymen’s Society, and The Univeristy of Alabama.

REFERENCES

Tsai, H. L., Chiang, K. C., Chen, T. S.; 1986, “Movement of Moisture Front and Alloy Solidification in Green Sand Casting,” AFS Transactions, pp. 191-196.

Marek, C. T., 1963, “Transformation Zones in Green Sand”, AFS Transactions, pp.185-192.

Marek, C. T., 1965, “Effect of Transformation Zones on Casting Problems.” AFS Transactions, pp. 134-141.

Chowdialh, M. P., 1973, “The Transport Zone and Its Movement in the Green Sand Mold Wall.” AFS Transactions, pp. 38-40.

Draper, A. B.,1969, “Condensation Zones in Molding Sands Bonded with Southern Bentonite”, AFS Transactions, vol. 77, pp. 407-414.

Kubo, K. et al ,1981, “Measurement of Thermal Properties of Various Sand Molds by Pouring Method with Aluminum”. AFS Transactions, pp. 311-318.

Beck, J. V, Blackwell Ben, and Clair Charles R. st.,1985, *Inverse heat conduction ill-posed problem*, Wiley, New York.

Beck, J. V, and Arnold, K. J., 1977, *Parameter Estimation in Engineering and Science*, Wiley, New York.

Junkins, J. L., 1978, *An Introduction to Optimal Estimation of Dynamical Systems*, Sijthoff & Noordhoff International Publishers.

Chen,Y., 1997, “ one dimensional non-linear sequential estimation of heat flux at casting /mold interface”, thesis for a master’s degree, the University of Alabama.

Press William H., Teukolsky Saul A. et al.,1993, *Numerical Recipes In C: The Art of Scientific Computing*, Cambridge University

Copyright © 1999 by ASME